Available online at www.sciencedirect.com
ScienceDirect
Biochemical and Biophysical Research Communications 354 (2007) 27–32
BBRC
www.elsevier.com/locate/ybbrc

Structural investigations on native collagen type I fibrils using AFM

Stefan Strasser [a,c], Albert Zink [a,c], Marek Janko [a,c], Wolfgang M. Heckl [a,b], Stefan Thalhammer [c,*]

[a] Department of Geo- and Environmental Sciences, Ludwig-Maximilians-Universität, 80333 Munich, Germany
[b] Deutsches Museum, Museumsinsel 1, 80538 Munich, Germany
[c] GSF-National Research Center for Environment and Health, Institute of Radiation Protection, AG Nanoanalytics, 85764 Neuherberg, Germany

Received 4 December 2006
Available online 22 December 2006

Abstract

This study was carried out to determine the elastic properties of single collagen type I fibrils with the use of atomic force microscopy (AFM). Native collagen fibrils were formed by self-assembly in vitro characterized with the AFM. To confirm the inner assembly of the collagen fibrils, the AFM was used as a microdissection tool. Native collagen type I fibrils were dissected and the inner core uncovered. To determine the elastic properties of collagen fibrils the tip of the AFM was used as a nanoindentor by recording force–displacement curves. Measurements were done on the outer shell and in the core of the fibril. The structural investigations revealed the banding of the shell also in the core of native collagen fibrils. Nanoindentation experiments showed the same Young's modulus on the shell as well as in the core of the investigated native collagen fibrils. In addition, the measurements indicate a higher adhesion in the core of the collagen fibrils compared to the shell.

Keywords: AFM; Microdissection; Force spectroscopy; Collagen

Collagen molecules consist of three polypeptide chains (α-chains), which form an unique triple-helical structure. More than 20 genetically distinct collagens exist in mammalian tissue, where collagen types I, II, III, V, and XI self-assemble into D-periodic cross-striated fibrils. Collagen molecules, forming the fibril, consist of an uninterrupted right handed triple helix called tropocollagen [1], approximately 300 nm in length and 1.5 nm in diameter. The collagen self-assembles in cross-striated fibrils that normally occur in the extracellular matrix of connective tissues. These fibrils are stabilized by covalent cross linking of specific lysines and hydroxolysines of the collagen molecules which are ordered parallel in a D-periodic pattern [2]. The stagger of molecules gives rise to a characteristic band pattern of light and dark regions when negatively stained and viewed using an electron microscope [3].

An improvement in the field of imaging molecular structures was accomplished by the invention of the Atomic Force Microscope (AFM) by Binnig et al. [4]. AFM investigations carried out by Paige et al. [5] show native fibrils and fibrous long spacing fibrils (FLS-fibrils) [6]. Cocoon-like fibrils, which are in the range of hundreds of nanometers in diameter and 10–20 mm in length, were found to coexist with mature FLS fibrils. On the basis of detailed AFM studies a stepwise process in the formation of FLS collagen was proposed. Gutsmann et al. [7] observed that collagen fibrils from tendons behave mechanically like tubes. They concluded that the collagen fibril is an inhomogeneous structure. Moreover, it was observed that high strain lead to molecular gliding within the fibrils and ultimately to a disruption of the fibril structure [8]. Automated electron tomography studies, performed on corneal collagen fibrils showed that collagen molecules are organized into microfibrils (≈4 nm diameter) in a 36 nm diameter collagen fibril, which are tilted at ≈15° to the fibril long axis

* Corresponding author. Fax: +49 89 3187 2942.
E-mail address: stefan.thalhammer@gsf.de (S. Thalhammer).

0006-291X/$ - see front matter © 2006 Elsevier Inc. All rights reserved.
doi:10.1016/j.bbrc.2006.12.114

in a right handed helix. Analysis of the lateral structure demonstrated that the microfibrils exhibit regions of order and disorder within the 67-nm axial repeat of the collagen fibrils [9].

AFM nanodissection of big FLS-fibrils with a width of about 1.7 μm and a banding pattern of 270 nm showed the FLS banding also in the core of the fibril [10]. For FLS-fibrils a different assembly pathway and structure are postulated. The characteristic banding mainly arises from the attachment of α1-acid glycoprotein in FLS-fibrils [11]. The characteristic banding of native fibrils is determined by the repetition of overlap and gap zones [12].

Several investigations using the AFM as a tool for measuring the tensile modulus of collagen fibrils and subunits revealed details in the protein assembly. Graham et al. calculated force elongation/relaxation profiles of single collagen fibrils using the AFM. The elongation profiles showed, that in vitro assembled human type I collagen fibrils are characterized by a large extensibility. It was shown that the fibrils are robust structures with a significant conservation of its elastic properties [13]. Gutsmann et al. probed the crosslinks on a lower level of organisation using an AFM cantilever to pull substructures out of the assembly. Two different rupture events were determined; the first with a strong bond and a periodicity of 78 nm (bonds between subunits) and a second weaker one with a periodicity of 22 nm (between molecules) [14]. Bozec and Horton [15] studied trimeric type I tropocollagen molecules by AFM, both topologically and by force spectroscopy, showing multiple stretching peaks on the molecular level similarly as shown by Gutsmann et al. [14]. Fratzl et al. and Puxkandl et al. [8,16] investigated the fibrillar structure, viscoelastic and mechanical properties of collagen by recording stress–strain curves. The stress–strain curves can be divided into several regions [28]. At first crimps [17] and kinks [18], are removed, before a linear region is seen where the collagen triple helices are stretched, along with increase of the gap zones compared with the overlap zones. Slippage is first seen within fibrils at crosslink deficient collagen [16], and then higher strains lead to a disruption of the fibril.

Here we used the AFM as a microdissection tool and a tool for probing local elasticity. The mechanical behaviour of native single fibrils was tested by recording force–distance curves on the shell and in the core of the fibrils to gain insights into the collagen assembly and mechanical properties.

Materials and methods

Preparation of the collagen fibrils. The collagen solution was prepared from calfskin (Sigma). Approximately 1 mg of the compound was dissolved in 1 ml of 0.5% acetic acid over night at 4 °C. The solution was sonicated for 1 h at 0 °C to dissolve any collagen aggregates. Finally, the mixture was centrifuged at 4000 rpm for 90 min at 4 °C and the supernatant was filtered through a 0.2 μm filter unit (Sigma), (modified protocol according Paige et al. [5]). The final dialysis mixture is composed of 0.5 mg/ml collagen, and 0.2 mg/ml α1-acid glycoprotein.

For the preparation a dialysis tubing (Serva, visking 8/32) with a molecular weight cut off (MWCO) of 12–14 kDa and a tube diameter of 6 mm was used. The received solution was diluted 10-fold after dialysis and dried in 10 μl aliquots on freshly cleaved mica. A detailed procedure for the dialysis procedure can be found in reference [19].

AFM microscopy. For morphological characterization a Topometrix Explorer (Atos, Germany) was used. It was operated in non-contact mode under ambient conditions, with 35% relative humidity, using NSC12 B (non-contact silicon cantilever) cantilevers (Mikromasch, Estonia). The spring constant of the non-contact probe (NSC) was 14 N/m. The resonant frequency of the NSC cantilever was 315 kHz. The nominal tip radius was specified <10.0 nm. Image analysis was performed using SPIP software (Image Metrology, Lyngby, Denmark).

AFM microdissection. To reveal the core of the collagen fibril, the AFM (Bioprobe, Park Scientific, USA) was used as a microdissection tool. For this the feedback of the z-piezo was switched off and the cantilever approached to the sample surface until the tip touched the sample. In order to apply the correct force to cut the fibril approximately in the upper half of the fibril diameter several pre-test were done using cantilevers with a spring constant of 56 N/m.

Force spectroscopy and data analysis. Elasticity measurements were carried out by recording force–distance curves using a NanoWizard AFM (JPK Instruments, Germany). Imaging and force spectroscopy were done in contact mode using CSC 37 A (nominal spring constant $k_c = 0.65$ N/m, nominal resonant frequency $f_R = 41$ kHz). The elasticity was measured both inside the fibril and on the outer shell at the same thickness of the sample. To evaluate the Young's moduli and the adhesion forces the force–displacement curves were processed using the software Microcal Origin and Microsoft Excel. To calculate the Young's moduli a suitable model has to be fitted to the contact region (above the zero line) of the force–distance curves. For the determination of the adhesion forces the height of the snap out of the retrace curve was calculated using the force spectroscopy data.

The indentation of an AFM tip into soft or hard samples can be modelled using the Hertzian contact mechanics [20]. The indentation of an infinitely hard body into a hard elastic half space (small indentations with the parabolic part of the tip) with a normal force F leads with this theory to [21–23]:

$$F_{\text{paraboloid}} = \frac{4}{3} \cdot \frac{E}{(1-\nu^2)} \cdot \delta^{3/2} \cdot \sqrt{R}, \tag{1}$$

where δ is the indentation depth, E is the Young's modulus, ν is the Poisson ratio and R is the tip radius. For incompressible materials the Poisson ratio is at 0.5. The applied force can be calculated with the deflection of the cantilever, which is considered as a tightened spring by Hook's Law:

$$F = k_c \cdot d, \tag{2}$$

where k_c is the spring constant and d is the deflection of the cantilever.

The deflection of the cantilever depends on the indentation of the tip into the elastic half space or rather the sample. The z-piezo extends and the distance of the extension z is split into the deflection and the indentation depth (δ) by

$$z = d + \delta \tag{3}$$

With these Eqs. (1)–(3) the Young's modulus can be expressed for hard samples as

$$E_{\text{paraboloid}} = \frac{3 \cdot k_c \cdot (d - d_0) \cdot (1-\nu^2)}{4 \cdot \sqrt{R} \cdot [(z - z_0) - (d - d_0)]^{3/2}}, \tag{4}$$

where d_o and z_0 are the corresponding values of the cantilever deflection and the z-piezo extension at the contact point. For soft samples in the contact regime Eq. (4) can be written as

$$z = \left[\frac{3 \cdot k_c \cdot (d - d_0) \cdot (1-\nu^2)}{4 \cdot E \cdot \sqrt{R}}\right]^{2/3} + (d - d_0) + z_0. \tag{5}$$

To calculate the Young's modulus, the model (Eq. (5)) was fitted to every recorded force–distance curve. The spring constant ($k_c = 0.7$ N/m) was determined by the Sader method [24,25], and the radius of curvature ($R \approx 20$ nm), defining the tip shape, was determined by SEM microscopy.

Results and discussion

AFM imaging and microdissection

For AFM microscopy the samples can be investigated immediately after self-assembly and drying on freshly cleaved mica. The described collagen preparation technique [19] allows the reproducible production of single collagen fibrils with different banding patterns (Fig. 1).

Thereby we were also able to detect collagen fibrils with kinks. Gutsmann et al. [7] suggested that this mechanical behaviour corresponds to a strong deformation of a tube. The combination of probing sample properties by doing force spectroscopy as well as the manipulation of the specimen with a high-resolution imaging tool is very useful in material characterization applications. The AFM as a nanoindentor proved its applicability for elasticity measurement and material classification in different applications [26,27]. We used the AFM to probe the sample properties of the centre and the surface of the fibril to compare the morphological investigations with directly measured mechanical values. The AFM based microdissection was applied to reveal the inner structure of the specimen. During manipulation the shell and upper parts of the fibril were scratched away, to image the remaining core in a high-resolution mode (Fig. 2). The dissection was carried out in a defined angle to the fibril axis in order to exclude artefacts originated by an orthogonal or parallel (to the fibril axis) scratching procedure. It could be shown

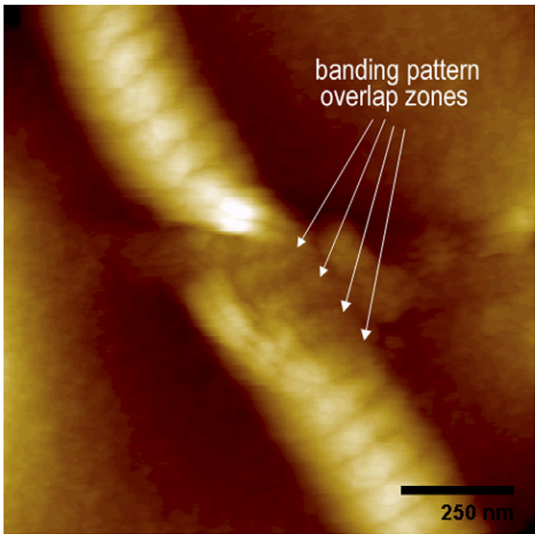

Fig. 2. High resolution AFM image of a microdissected collagen fibril. The core of the collagen fibril is revealed and the banding pattern can be recognized inside the fibril. The arrows indicates the overlap zones of the collagen molecules that arise during the self-assembly process of the collagen fibril (topography signal, scalebar 250 nm).

that there are no major geometrical differences of the banding on the shell and in the core of native single collagen fibrils. The banding pattern inside the fibril fits to that on the shell in width and distance. The fibril has a banding pattern of 78 nm, a height of 30 nm, and a width of 270 nm. The cutted area, shown in Fig. 2, is located in the core of the fibril, which was confirmed by line measurements (Fig. 3). Between the measured distance A and B the banding can be recognized on the shell as well as in the core. Among points C and D the height difference between

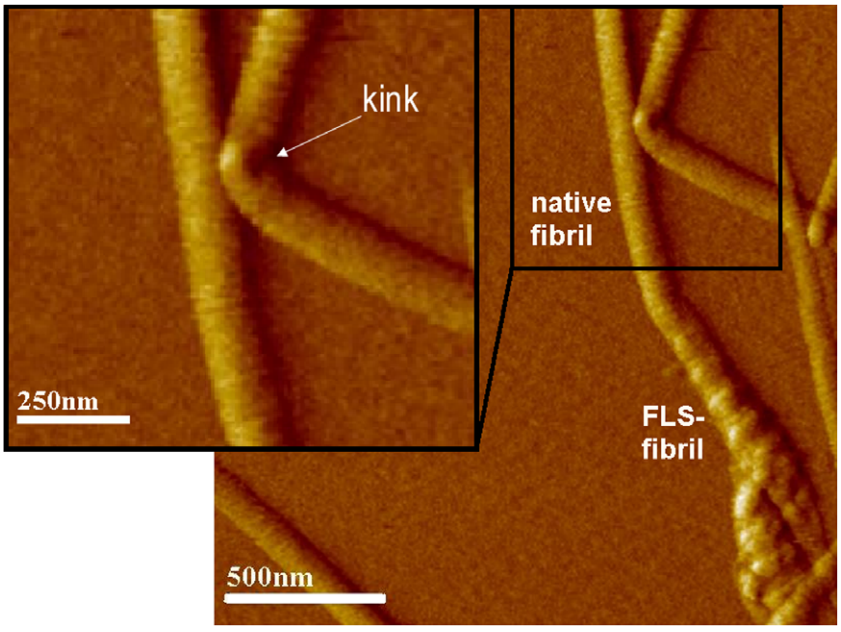

Fig. 1. High resolution AFM image of a single collagen fibril with kink. Due to kinks collagen are sometimes compared to tubes. The other fibril displays the polymorphism of collagen with native and FLS-parts in one fibril (error signal, scalebar 500 nm).

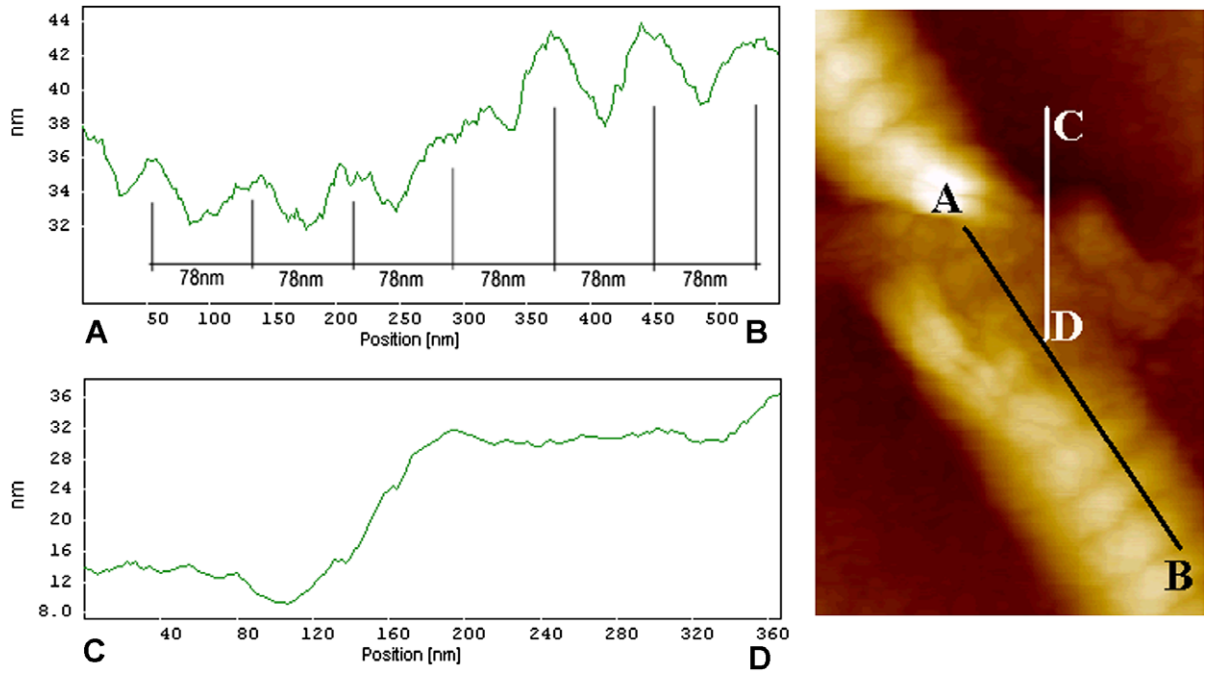

Fig. 3. Line measurements on the microdissected collagen fibril (Fig. 2). Between point A and B the banding can be recognized on the shell as well as in the core. The banding pattern can be determined to be approximately 78 nm. Between point C and D the height difference of around 16 nm between the substrate and the level of the cut area can be seen.

the substrate and the level of the cut area can be seen. The height difference between the substrate and cut area was determined to be 16 nm. These results are in concordance with Wen and Goh [10] who also showed a similar morphological structure of core and shell in FLS-fibrils, with a different assembly pathway and structure compared to native single collagen fibrils [11]. In a recently published work they further confirmed the differences of FLS fibrils to native collagen fibrils on the base of the superhelical structure and hierarchical organisation of disrupted fibrils [28]. Based on the model, that aligned tropocollagen molecules build the mature fibril by crosslinking with neighbour molecules in native collagen fibrils [14], it has to be taken into consideration that during microdissection complete layers are removed (Fig. 2). However, the scratching process can lead to a rupture of molecules and destruction of crosslinking. Different elastic properties of core and shell could be generated during the manipulation process. This is a major problem when probing inhomogeneous biological samples in the molecular range and influences during manipulation could not be completely excluded.

Force spectroscopy

For core and shell, respectively, more than 100 force–distance curves were recorded. The displayed data are representative for several experiments. The indentation depth on both areas was limited with a set-point-force for every force–distance curve. The maximal force of about 6 nN, corresponding to a cantilever bending of 8.5 nm, led to an indentation depth of about 0.5 nm both on the shell and core of the fibril. Exemplary force–distance curves recorded on the shell and the core are displayed in Fig. 4A. The dark curve shows a spectroscopy curve on the shell, whereas the grey dashed curve was recorded in the core. The indentation experiments were repeatedly performed on several collagen fibrils. The slope of both curves recorded on the shell and the core showed no major differences indicating a comparable elasticity. The evaluation of the spectroscopy data was done at the positive cantilever deflection range above the zero line. The histogram in Fig. 4B displays the Young's moduli of the force–distance curves. The Young's moduli were calculated applying a fit of the Hertzian model to the contact range of the individual force–distance curves. The average values indicate no significant difference in elasticity between core and shell. The indentation experiments, performed on the shell and the core of dissected collagen fibrils could not verify different Young's moduli of core and shell. This is also well in line with our morphological results in Fig. 2 which shows a homogeneous assembly of the fibril. The average values were calculated to approximately 1.2 Gpa. The maximum of the distribution lies at 1 GPa. The results of indentation experiments of thin samples can also be influenced by the underlaying hard substrates. Samples can be compressed under the tip and the measured Young's modulus is maybe upper estimated, shown by Domke et al. [23]. In order to avoid this effect, the force curves were recorded on areas with the same sample height. It is also likely possible that the sample preparation especially the α1-acid glycoprotein concentration influences the mechanical properties of the collagen fibrils. It was proposed that proteoglycans have

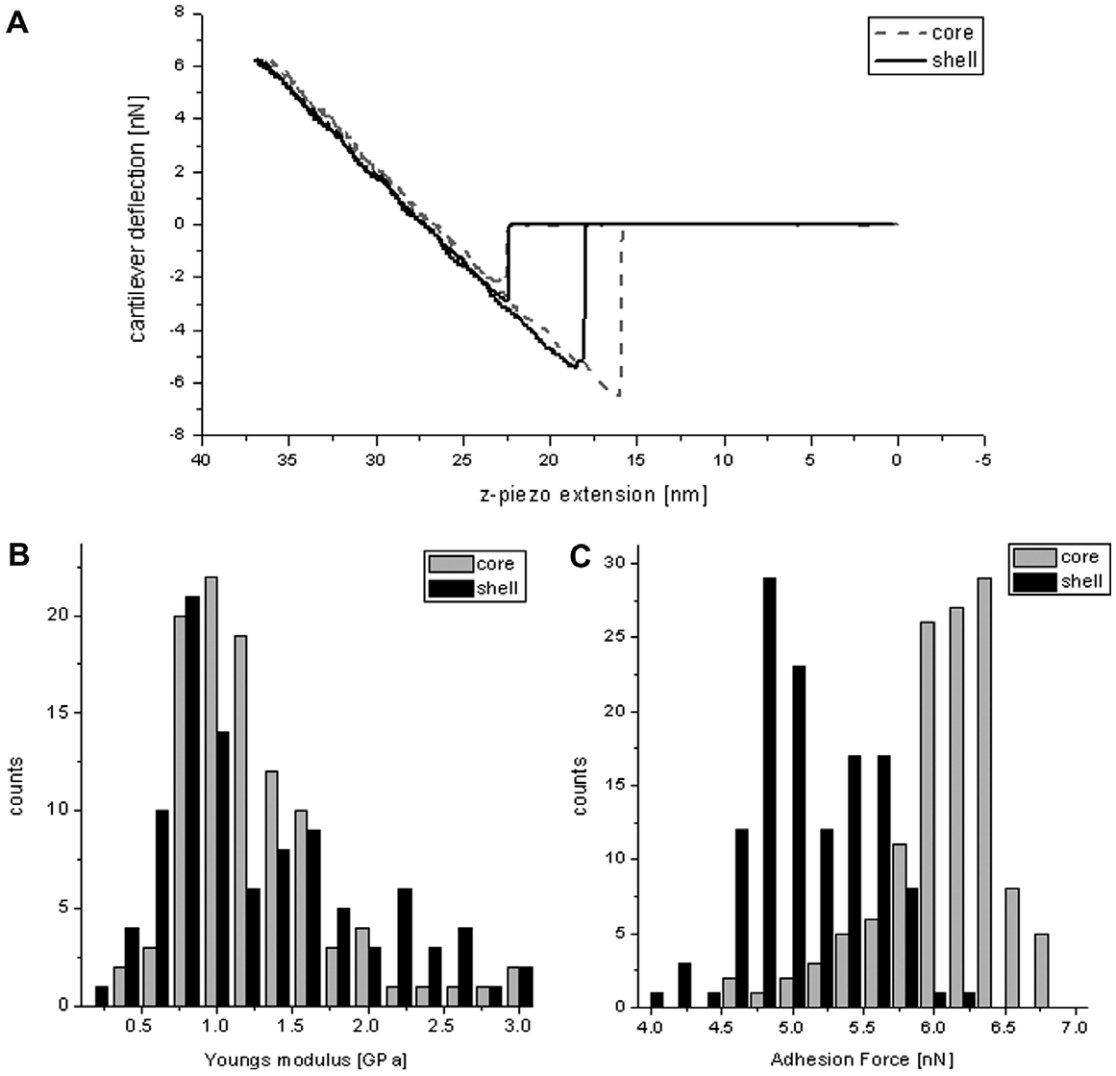

Fig. 4. (A) Typical sample of a force–distance curves recorded on the shell and the core of a single collagen fibril. The dark curve shows a spectroscopy curve on the shell, whereas the grey dashed curve was recorded in the core. The slope of both curves is nearly the same and indicates identical elasticity. Measurements on the shell and in the core have to be performed in the same sample height to exclude ''thin layer effects''. The Hertzian model was fitted to the positive cantilever deflection range. (B) Elasticity measurement of a single collagen fibril. Force distance curves were recorded on the shell and the exposed core. On both measuring points more than 100 curves were recorded. The diagram displays the Young's moduli of the force distance curves versus the frequency. The nanoindentation experiment indicates no measurable difference between core and shell. (C) Adhesion measurement on a single collagen fibril. The data display the evaluation of the adhesion forces calculated from the height of the snap out of the retrace curve, see also the figure. The values show a higher adhesion in the core of the microdissected fibril.

an important influence on mechanical properties of the fibrils [7]. This could explain the difference between the measured and the literature value of 1 GPa [29]. Since the same cantilever was used for both sets of force curves, the comparison between core and shell is still valid.

The evaluation of the adhesion forces of the spectroscopy data indicates a higher adhesion in the core of the fibril. This can be already seen in Fig. 4A where typical spectroscopy data for core and shell are displayed. In Fig. 4C the height of the snap out effect calculated from the retrace curves is shown. The average value was calculated for the shell to 5 nN and for the core to 6 nN which points to a higher adhesion in the core of the fibril. Gutsmann et al. [7] suggested the presence of more highly crosslinked collagen molecules near the fibril surface compared to the central region. This could lead to a higher amount of binding capacity for the tip and cause higher adhesion forces during the measurement. However, the results could have been also influenced by the scratching process which could have led to a rupture of molecules and destruction of crosslinks. The destroyed crosslinks and ruptured molecules could stick to the tip and increase the measured adhesion force. Moreover, the collagen fibrils were investigated in a dried state of preservation, which could have also an influence on the mechanical properties.

The mechanical properties of this collagen rich tissues, e.g., tendons, are largely determined by the collagen structure [8]. An inhomogeneous assembly of collagen fibrils

was published by several authors; Sarkar et al. [30] proposed that fluid domains in the collagen allow molecules to slip relative to one another, which was shown by Mosler et al. [31], in order to relieve applied stress. It has been proposed that, in case of high forces, the stiff outer shell of the collagen fibrils could break while the fluid core remains intact and might be used in the repair of the shell [7]. Our morphological results as well as the statistical evaluation of the Young's modulus using the indentation measurements could not confirm a ''fluid'' core or different structures of core and shell. Solely the adhesion measurements show differences between core and shell.

Acknowledgments

We thank Prof. Dr. Achim Wixforth, Dr. Matthias Schneider, and Daniel Steppich for their help and opportunity to perform the force spectroscopy measurements at the Lehrstuhl für Experimentalphysik II of the University of Augsburg.

References

[1] G.N. Ramachandra, G. Karthan, Structure of collagen, Nature 176 (1955) 593–595.
[2] K.E. Kadler, D.F. Holmes, J.A. Trotter, J.A. Chapman, Collagen fibril formation, Biochem. J. 316 (1996) 1–11.
[3] B.R. Williams, R.A. Gelman, D.C. Poppke, K.A. Piez, Collagen fibril formation, J. Biol. Chem. 253 (1978) 6578–6585.
[4] G. Binnig, C.F. Quate, C. Gerber, Atomic force microscope, Phys. Rev. Lett. 56 (1986) 930–933.
[5] M.F. Paige, J.K. Rainey, M.C. Goh, Fibrous long spacing collagen ultrastructure elucidated by atomic force microscopy, Biophys. J. 74 (1998) 3211–3216.
[6] V.J. Morris, A.R. Kirby, A.P. Gunning, Atomic Force Microscopy for Biologists, Imperial College Press, London, 1999. ISBN:1860941990.
[7] T. Gutsmann, G.E. Fantner, M. Venturoni, A. Ekani-Nkodo, J.B. Thompson, J.H. Kindt, D.E. Morse, D.K. Fygenson, P.K. Hansma, Evidence that collagen fibrils in tendons are inhomogeneously structured in a tubelike manner, Biophys. J. 84 (2003) 2593–2598.
[8] P. Fratzl, K. Misof, I. Zizak, G. Rapp, H. Amenitsch, S. Bernstorff, Fibrillar structure and mechanical properties of collagen, J. Struct. Biol. 122 (1998) 119–122.
[9] D.F. Holmes, C.J. Gilpin, C. Baldock, U. Ziese, A.J. Koster, K.E. Kadler, Corneal collagen fibril structure in three dimensions: Structural insights into fibril assembly, mechanical properties, and tissue organization, Proc. Natl. Acad. Sci. USA 98 (2001) 7307–7312.
[10] C.K. Wen, M.C. Goh, AFM nanodissection reveals internal structural details of single collagen fibrils, Nano. Lett. 4 (2004) 129–132.
[11] J.K. Rainey, C.K. Wen, M.C. Goh, Hierarchical assembly and the onset of banding in fibrous long spacing collagen revealed by atomic force microscopy, Matrix Biol. 21 (2002) 647–660.
[12] J.A. Petruska, A.J. Hodge, Subunit model for tropocollagen macromolecule, Proc. Natl. Acad. Sci. USA 51 (1964) 871–876.
[13] J.S. Graham, A.N. Vomund, C.L. Phillips, M. Grandbois, Structural changes in human type I collagen fibrils investigated by force spectroscopy, Exp. Cell Res. 299 (2004) 335–342.
[14] T. Gutsmann, G.E. Fantner, J.H. Kindt, M. Venturoni, S. Danielsen, P.K. Hansma, Force spectroscopy of collagen fibers to investigate their mechanical properties and structural organization, Biophys. J. 86 (2004) 3186–3193.
[15] L. Bozec, M. Horton, Topography and mechanical properties of single molecules of type I collagen using atomic force microscopy, Biophys. J. 88 (2005) 4223–4231.
[16] R. Puxkandl, I. Zizak, O. Paris, J. Keckes, W. Tesch, S. Bernstorff, P. Purslow, P. Fratzl, Viscoelastic properties of collagen: synchrotron radiation investigations and structural model, Philos. Trans. R. Soc. Lond. B Biol. Sci. 357 (2002) 191–197.
[17] J. Diamant, R.G.C. Arridge, E. Baer, M. Litt, A. Keller, Collagen—ultrastructure and its relation to mechanical properties as a function of aging, Philos. Trans. R. Soc. Lond. B Biol. Sci. 180 (1972) 293–315.
[18] P. Fratzl, N. Fratzlzelman, K. Klaushofer, Collagen packing and mineralization—an X-ray-scattering investigation of turkey leg tendon, Biophys. J. 64 (1993) 260–266.
[19] S. Strasser, A. Zink, W.M. Heckl, S. Thalhammer, Controlled self-assembly of collagen fibrils by an automated dialysis system, J. Biomech. Eng. (2006).
[20] H. Hertz, Über die Berührung fester elastischer Körper, J. Reine angewandte Mathematik 92 (1882) 156–171.
[21] I.N. Sneddon, The relation between load and penetration in the axisymmetric Boussinesq problem for a punch of arbitrary profile, Int. J. Eng. Sci. 3 (1965) 47–57.
[22] K.L. Johnson, Contact Mechanics, Cambridge University Press, Cambridge, 1994. ISBN-13: 9780521347969.
[23] J. Domke, M. Radmacher, Measuring the elastic properties of thin polymer films with the atomic force microscope, Langmuir 14 (1998) 3320–3325.
[24] J.E. Sader, J.W.M. Chon, P. Mulvaney, Calibration of rectangular atomic force microscope cantilevers, Rev. Sci. Instrum. 70 (1999) 3967–3969.
[25] J.L. Hutter, J. Bechhoefer, Calibration of atomic-force microscope tips, Rev. Sci. Instrum. 64 (1993) 1868–1873.
[26] J.B. Thompson, J.H. Kindt, B. Drake, H.G. Hansma, D.E. Morse, P.K. Hansma, Bone indentation recovery time correlates with bond reforming time, Nature 414 (2001) 773–776.
[27] S. Strasser, A. Zink, G. Kada, P. Hinterdorfer, O. Peschel, W.M. Heckl, A.G. Nerlich, S. Thalhammer, Age determination of blood spots in forensic medicine by force spectroscopy, Forensic Sci. Int. (2006), doi:10.1016/j.forsciint.2006.1008.1023.
[28] C.K. Wen, M.C. Goh, Fibrous long spacing type collagen fibrils have a hierarchical internal structure, proteins: structure, Funct. Bioinform. 64 (2006) 227–233.
[29] Y.C. Fung, Biomechanics—mechanical properties of living tissue, second ed., Springer, New York 1993. ISBN: 0387979476.
[30] S.K. Sarkar, Y. Hiyama, C.H. Niu, P.E. Young, J.T. Gerig, D.A. Torchia, Molecular-dynamics of collagen side-chains in hard and soft-tissues—a multinuclear magnetic-resonance study, Biochemistry-Us 26 (1987) 6793–6800.
[31] E. Mosler, W. Folkhard, E. Knorzer, H. Nemetschekgansler, T. Nemetschek, M.H.J. Koch, Stress-induced molecular rearrangement in tendon collagen, J. Mol. Biol. 182 (1985) 589–596.